

ON STATIC STABILITY OF NONLINEARLY ELASTIC EULER'S COLUMNS OBEYING THE MODIFIED LUDWICK'S LAW

MIHA BROJAN*, MATEJ SITAR and FRANC KOSEL

*Laboratory for Nonlinear Mechanics
Faculty of Mechanical Engineering
University of Ljubljana, Askerceva 6, SI-1000
Ljubljana, Slovenia
miha.brojan@fs.uni-lj.si

Received 27 May 2011
Accepted 31 October 2011
Published 31 December 2012

It is illustrated in this paper that a nonlinearly elastic column, depending upon the values of different material parameters involved, exhibits several stability characteristics and types of buckling which are generally observed separately in distinctively different structural systems. By introducing finite disturbances it is shown that the column may buckle well before the bifurcation buckling load is reached. The proposed approach can be useful in engineering practice since it can be utilized to study the stability of uniaxial structural elements made from rubber or any other material which obeys the modified Ludwick's constitutive model.

Keywords: Post-buckling; stability; bifurcation buckling; finite-disturbance buckling; limit-point buckling; nonlinear elasticity; modified Ludwick's constitutive model.

1. Introduction

Buckling or instantaneous collapse of structural systems caused by external and/or internal loads, not sufficient to cause yield in the material of the structure, has been treated extensively in the existing literature, especially Euler's elastica. At first, it was shown that bifurcation point divides the solution domain into pre- and post-critical sub-domains; where the first sub-domain is stable and corresponds to a trivial solution (initially straight column configuration), while the latter is either unstable (trivial solution) or stable which corresponds to a deformed column. Subsequently it was shown that the nontrivial branch of solution in the post-critical sub-domain is not stable entirely. For example, Wang¹ analyzed the complete post-buckling sub-domain of clamped–simply supported elastica and discovered that the bifurcation

*Corresponding author.

curve of the nontrivial post-critical branch is not monotonic. He found a limit point and thus showed that post-buckling behavior exhibits further nonlinear phenomena such as snap-through which results in so-called secondary loss of stability. Studies done by Korobeinikov,² Kuznetsov and Levyakov,^{3–6} and similarly Wu^{7–9} have also revealed previously unknown bifurcation points and solution branches.

Following these results, in the present paper Euler’s elastica is generalized to the context of nonlinearly elastic material with the main focus on analysis of stability conditions. The topic of global stability of a special case, a clamp–free supported column was treated by Wang, cf. Ref. 10, where material nonlinearity was introduced through the relation between inner bending moment and curvature. Similar problem was addressed by Kang *et al.*¹¹ They investigated bending and stability of a clamp–clamp supported column fiber. Jung and Kang¹² also analyzed deflections of a column fiber but in their case constitutive equation corresponded to a Ludwick or modified Ludwick type. They presented deflection diagrams for four different combinations of a horizontal and vertical direction of point and distributed load. Analysis of global stability and post-buckling behavior of a clamped–free columns made from Ludwick-type nonlinearly elastic material was studied by Brojan *et al.*¹³ Furthermore, approximative formulas for clamp–free, hinge–hinge and clamp–clamp supported nonlinearly elastic columns in post-buckling domain were developed by Brojan and Kosel¹⁴ to study stability conditions and deflections.

It will be shown here, that this relatively simple model is interesting for structural stability studies because, depending upon the values of different material parameters involved, it exhibits various types of buckling generally observed separately in distinctively different structural systems, including bifurcation buckling, limit-point buckling, and finite-disturbance buckling.

2. Problem Statement

Consider a slender, initially straight elastic column of length L and uniform rectangular cross-section of thickness h and width b . The column with various supports is subjected to an axial force P in compression, Fig. 1. As this force exceeds a certain value P_{cr} the column may deflect laterally, as shown in Figs. 1(b) to 1(e).

By δ ,

$$\delta = L - \int_0^L \cos \vartheta(s) ds, \quad (1)$$

vertical displacement of the column is denoted.

The material of which the Euler’s columns are made is assumed to be incompressible, homogenous, isotropic, and nonlinearly elastic. It follows the modified Ludwick’s constitutive model, mathematically described by the following expression

$$\sigma(\varepsilon) = \text{sign}(\varepsilon) E [(|\varepsilon| + \varepsilon_0)^{1/k} - \varepsilon_0^{1/k}], \quad (2)$$

where E , k , and ε_0 represent material constants, cf. Refs. 12 and 15.

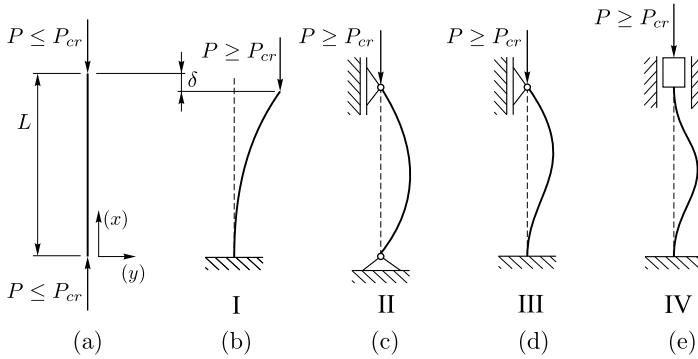


Fig. 1. Trivial and post-critical shape modes of the Euler's columns.

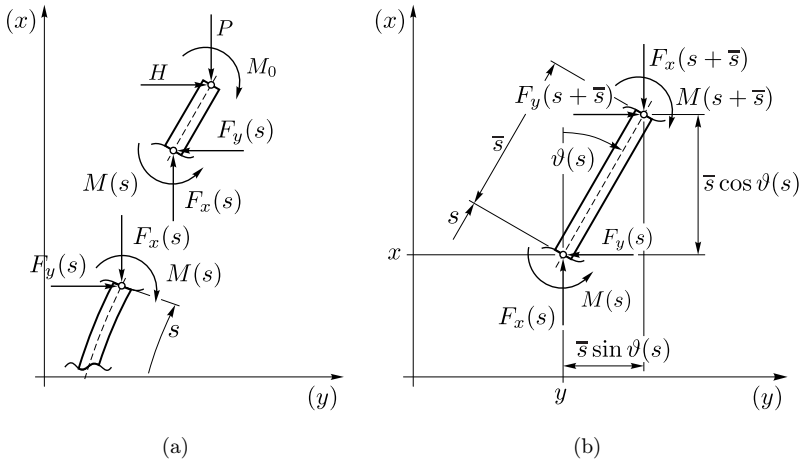


Fig. 2. Deformed configuration and infinitesimal element of the deflected column.

The Cartesian coordinate system is introduced such that the x -axis coincides with the longitudinal axis of the undeformed column and the coordinate origin is located at its fixed end. Let $s, 0 \leq s \leq L$, be the curvilinear coordinate along the longitudinal axis of the column measured from the fixed end and $\vartheta(s)$ the angle of inclination at local point s , see Fig. 2.

Static equilibrium of the column segment, Fig. 2(a) where H and M_0 represent reactive force and moment acting in the support of the column, and static equilibrium of an infinitesimal element, Fig. 2(b), together with geometrical relations,

$$x'(s) = \cos \vartheta(s) \quad \text{and} \quad y'(s) = \sin \vartheta(s), \quad (3)$$

yields

$$M'(s) + P \sin \vartheta(s) + H \cos \vartheta(s) = 0. \quad (4)$$

From the expression for the inner bending moment $M = -\int_A \sigma y dA$, material constitutive model described by Eq. (2), and normal strain-curvature expression $\varepsilon = -y\rho^{-1}$ which is a reasonable approximation for sufficiently slender columns, one can deduce

$$M(s) = 2bkE\rho(s)^2 \left[\frac{(1+k)h \mp 2k\varepsilon_0\rho(s)}{2(1+k)(1+2k)\rho(s)} \left(\frac{\pm h}{2\rho(s)} + \varepsilon_0 \right)^{1+1/k} \pm \frac{k\varepsilon_0^{2+1/k}}{(1+k)(1+2k)} \mp \frac{h^2\varepsilon_0^{1/k}}{8k\rho(s)^2} \right], \quad (5)$$

where $\rho(s)$ represents the radius of the column's curvature at point s , cf. Ref. 15. The upper symbol in \pm, \mp designates the sign in case of positive curvature and vice versa. Finally, substituting geometrical relation $\rho^{-1}(s) = \vartheta'(s)$ and Eq. (5) into Eq. (4) leads to the governing differential equation of the problem,

$$-\frac{\vartheta''(s)}{(\vartheta'(s))^3} \left[\pm A\varepsilon_0^{1/k} \pm \left(\varepsilon_0 \pm \frac{h}{2} \vartheta'(s) \right)^{1/k} (-A \pm B\vartheta'(s) - C(\vartheta'(s))^2) \right] + P \sin \vartheta(s) + H \cos \vartheta(s) = 0, \quad (6)$$

where $'$ denotes differentiation with respect to variable s and A, B, C are introduced quantities

$$A = \frac{4bEk^2\varepsilon_0^2}{(1+k)(1+2k)}, \quad B = \frac{Ah}{2k\varepsilon_0}, \quad C = \frac{bEh^2}{2(1+2k)}. \quad (7)$$

Equation (6) together with the accompanying boundary conditions characterizes the post-buckling behavior of columns subjected to an axial force. Boundary conditions and bifurcation loads of the columns investigated in this paper are listed in Table 1. The values of the bifurcation loads can be obtained via linearization of the problem. They are the solutions of the well known transcendental equations, $\cos \omega = 0$, $\sin \omega = 0$, $\omega - \tan \omega = 0$ and $\omega \sin \omega + 2 \cos \omega - 2 = 0$, where $\omega = L\sqrt{P_{\text{bif}}(E_m I)^{-1}}$. Linearization of the modified Ludwick's stress-strain relationship at small strains, e.g. yields

$$E_m := \left. \frac{d\sigma}{d\varepsilon} \right|_{\varepsilon=0} = \frac{\varepsilon_0^{\frac{1-k}{k}} E}{k}. \quad (8)$$

Table 1. Boundary conditions and bifurcation loads.

Euler case	Support	Boundary conditions		$P_{\text{bif}} \cdot L^2 / (E_m I)$
I	Clamp-free	$\vartheta(0) = 0,$	$\vartheta'(L) = 0$	$\pi^2/4$
II	Hinge-hinge	$\vartheta'(0) = 0,$	$\vartheta'(L) = 0$	π^2
III	Clamp-hinge	$\vartheta(0) = 0,$	$\vartheta'(L) = 0$	$\doteq 2.0457\pi^2$
IV	Clamp-clamp	$\vartheta(0) = 0,$	$\vartheta(L) = 0$	$4\pi^2$

Constant E_m corresponds to the elastic modulus of a linearly elastic (Hooke's) material which has approximately the same response as modified Ludwick's material at small strains. This approximation may often be useful when e.g. determining bifurcation buckling force.¹⁵

The governing second order nonlinear differential equation is solved numerically using the Runge–Kutta–Fehlberg (RKF) integration method. Boundary value problem is converted to initial value problem by employing parameter $\mu := \vartheta'(0)$ and solved using shooting method. At fixed value of the force P , force H is unknown in the III Euler's case. Therefore additional condition $y(L) = 0$ is taken into account. Since there are two unknown parameters in the numerical procedure, i.e. μ and H , Newton's method for system of nonlinear equations is applied. Furthermore, the Cartesian coordinates of the points along the natural axis of the column can be determined from the geometrical relations (3) and boundary conditions $x(s = 0) = 0, y(s = 0) = 0$.

3. Examples and Discussion

Based on the mathematical model presented above, a complete stability analysis of all four Euler's cases for three types of material, i.e. linearly elastic, softening-elastic, and hardening-elastic material, is shown in this section. Geometrical properties of the column are length $L = 500.0$ mm, width $b = 50.0$ mm and thickness $h = 15.0$ mm. Particular values of material parameters used in numerical calculations can be found in Fig. 3.

Static stability analysis of structures is crucial when multiple equilibrium states (which are not necessarily infinitesimally close) exist at a certain value of the load, i.e. when equilibrium can be achieved with two or more different deformation

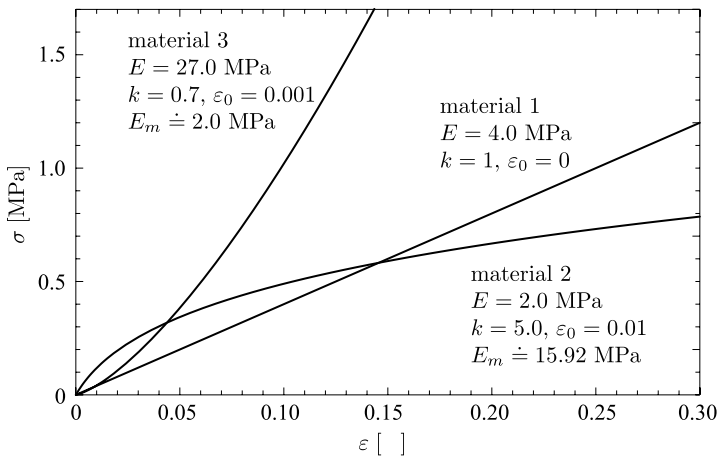


Fig. 3. Stress–strain relations and material parameters.

configurations at the same level of the load. We will denote a system in (quasi) static equilibrium as in (i) *neutral*, (ii) *unstable*, (iii) (*locally*) *stable* or (iv) *globally stable* state:

- (1) if there exists exactly one equilibrium configuration;
- (2) if even infinitesimal disturbance is sufficient for a system to pass to a different equilibrium configuration;
- (3) if only *finite* disturbance is sufficient for a system to pass to a different equilibrium configuration;
- (4) if even finite disturbance cannot incite a system to pass to a different equilibrium configuration,

respectively. By disturbance we mean arbitrary transient load or displacement. A disturbance can be, as already mentioned, of infinitesimal or finite magnitude.

In general, there are three different ways by which the new equilibrium configuration may be reached;

- (a) by *classical* or *bifurcation* buckling, which occurs when the load is (quasistatically) increased beyond a certain level (bifurcation point) causing that an infinitesimally disturbed structure passes from one (unbuckled) equilibrium state to a distinctively different (buckled) equilibrium configuration. A sudden change of shape of the structure is characteristic for this type of buckling, e.g. change from axial contraction to lateral deflection of an axially loaded column in compression;
- (b) by *finite-disturbance* buckling, which occurs only when a finite disturbance makes the structure pass between two (not infinitesimally close) equilibrium configurations. Typical examples of such buckling is buckling of a thin cylindrical shell under axial compression or buckling of a complete, spherical, thin shell under uniform external pressure, cf. Ref. 16;
- (c) and by a third type of buckling which is known as *snap-through* or *limit-point* buckling when the load is increased infinitesimally beyond the critical level (limit point). This phenomenon is characterized by a sudden jump from one equilibrium configuration to another for which displacements are only larger than in the first configuration, i.e. they do not change the course of deformation as do in the case of classical buckling. Typical examples of this type are snapping of low, pinned arch under lateral load and snapping of a clamped shallow spherical cap under uniform lateral pressure, cf. Ref. 16.

It is illustrated below that a nonlinearly elastic column, depending upon the values of different material parameters involved, exhibits all the mentioned stability characteristics and types of buckling, which are generally observed separately in distinctively different structural systems. The results of the numerical calculations are accurate to within 10^{-6} .

3.1. I Euler's case

As will be illustrated in the figures below, the equilibrium solution is always unique for a given displacement whereas for a given load multiple equilibrium solution exists. The graph of characteristic (stability) function which is represented by relation between the load P and vertical displacement δ , cf. Eq. (1), Fig. 1, of the column's free end during bending, is shown in Fig. 4.

In a linearly elastic material case, i.e. material one ($k = 1, \varepsilon_0 = 0$), the well-known force–displacement curve is found, Fig. 4(a). The critical buckling force which is in this case equal to the bifurcation load is calculated to be at $P_{cr} = P_{bif} = 0.555$ N. Detailed explanation of the stability conditions and all special points in Fig. 4(a) to 4(c) is given in the text below, more specifically in Sec. 3.2.

The bifurcation buckling force in the first nonlinearly elastic material case, i.e. material two ($k > 1, \varepsilon_0 \neq 0$), is $P_{bif} = 2.210$ N and the (global) critical buckling force $P_{cr} = 1.608$ N. By setting $\varepsilon_0 = 0$ and thereby simplifying the rheological model (2) to the case of Ludwick's model, leads to the same problem as has been partially treated in Refs. 13 and 14.

The bifurcation buckling force was computed also for the second nonlinearly elastic material case, i.e. material 3 ($k < 1, \varepsilon_0 \neq 0$), and is $P_{bif} = 0.277$ N = P_{cr} . Note also that numerically obtained values for bifurcation loads are the same as those obtained via formulas from Table 1.

Stable and unstable post-buckling shape modes for all three configurations of material constants are depicted in Fig. 5 for I Euler's case.

Post-buckling shape modes, depending upon the values of different material parameters involved, for this clamped–free column are shown in Fig. 6 at constant

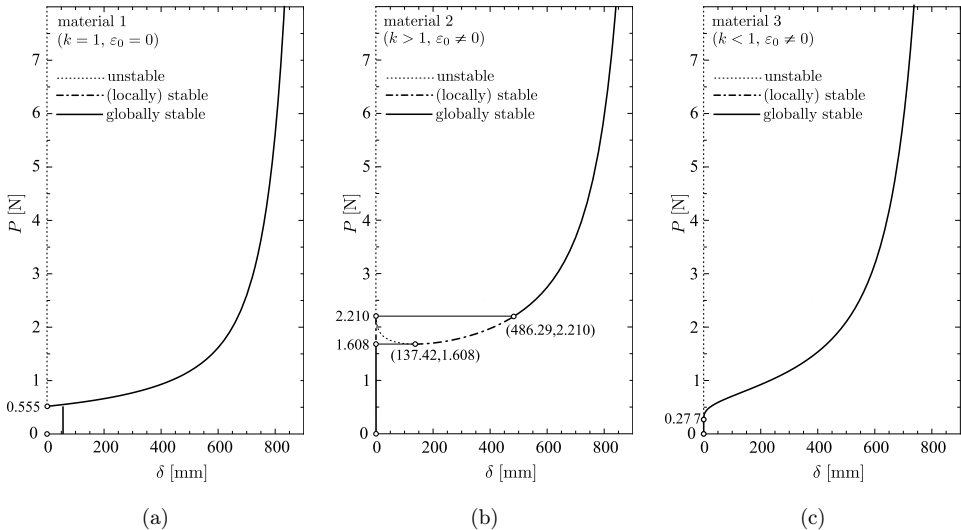


Fig. 4. Characteristic P – δ curves for I Euler's case.

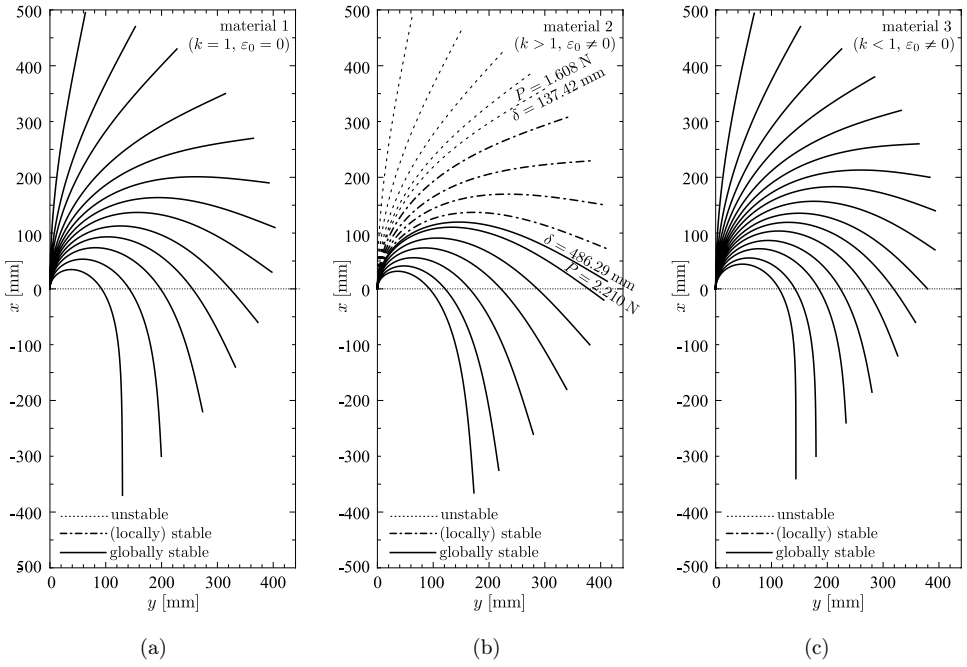


Fig. 5. Stable and unstable post-buckling shape modes for I Euler's case.

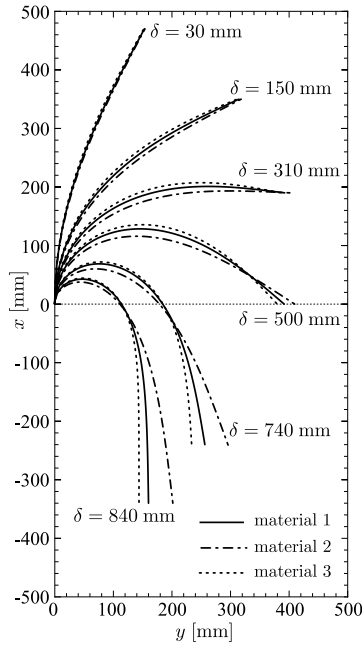


Fig. 6. Comparison of post-buckling shape modes for I Euler's case.

values of characteristic displacement $\delta = 30$ mm, $\delta = 150$ mm, $\delta = 310$ mm, $\delta = 500$ mm, $\delta = 740$ mm, and $\delta = 840$ mm.

3.2. II Euler's case

Results comparable to those in the previous case are obtained as expected for the II Euler's case. Practically the same shapes of $P-\delta$ curves can be observed in Fig. 7.

In a linearly elastic material case, material one ($k = 1, \varepsilon_0 = 0$), cf. Fig. 7(a), the well known force-displacement curve is found. A neutral equilibrium is maintained on segment **0A** as load P quasistatically increases from **0** to point **A** where bifurcation occurs, $P_{cr} = P_A = 2.220$ N. As P is increasing, two equilibrium solutions are found in the post-buckling sub-domain, one globally stable on **(A)BI** branch, and one unstable solution on **(A)CJ** branch which corresponds to a straight column configuration. Here, designatiozn **(A)** means that point **A** itself is excluded from the segments **ABI** and **ACJ**. The $P-\delta$ curve of the nontrivial post-critical branch is monotonic, since $dP/d\delta > 0$ for all positive δ . As P is decreasing gradually from **I**, the unloading path **IBA0** is obtained. The loading and unloading paths, **0ABI** and **IBA0**, respectively, are thus the same. In addition, if during loading no disturbance is applied up to point **C** the column passes from unstable state at **C** to globally stable state **B**. The loading and unloading paths are thus different; namely **0ACBI** and **IBA0**, respectively.

One of the most important results in the present paper refers to the analysis of the nonlinear material case, (softening-elastic material 2, $k > 1, \varepsilon_0 \neq 0$ and hardening-elastic material 3, $k < 1, \varepsilon_0 \neq 0$). In the first nonlinear material case, Fig. 7(b) shows that the nontrivial part of the characteristic curve $P-\delta$ is not monotonic. Namely,

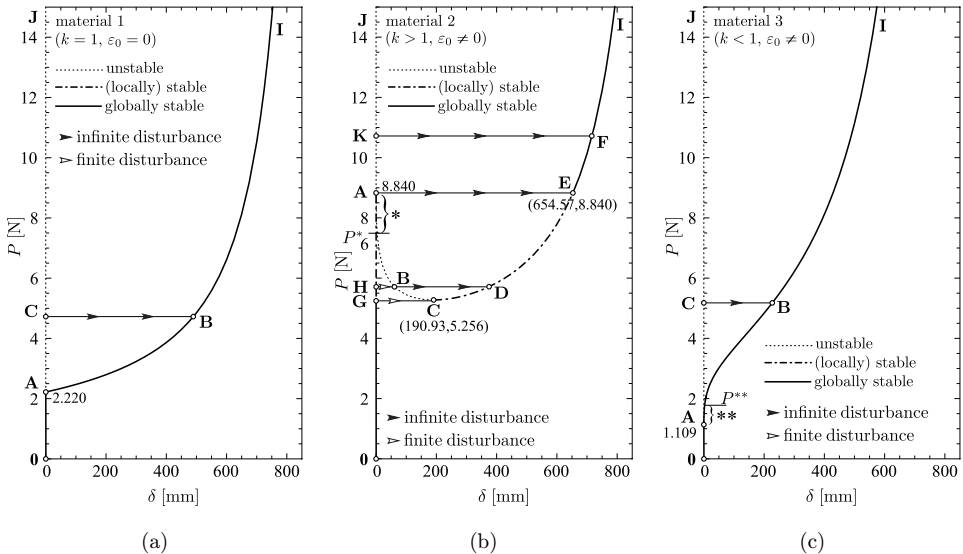


Fig. 7. Characteristic $P-\delta$ curves for II Euler's case.

for a positive displacement increment δ , the load P is decreasing on the **ABC** segment, but increasing on the **CDEFI** segment of the path. Clearly, since the area under the characteristic P - δ curve represents the work done on the elastica, this means a negative slope ($dP/d\delta < 0$) of the curve signifies negative work and thus statically unstable equilibrium state for a given constant load, and a positive slope ($dP/d\delta > 0$) positive work and statically (locally) stable equilibrium state.¹ The proof can be found e.g. in work done by Maddocks.¹⁷ Point **C** is the local minimum of the P - δ curve. Bifurcation buckling force $P_{\text{bif}} = P_A = 8.840$ N is found at bifurcation point **A** which divides the curve of equilibrium states into the unstable branch **AKJ** (trivial solution) and the branch which is unstable on the **ABC** segment, locally stable on the **(C)D(E)** segment and globally stable on the **EFI** segment. It is observed that the pre-critical sub-domain **OGHA** is in neutral state only for $P < P_G = 5.256$ N, i.e. in **0(G)** segment. In segment **(G)H(A)**, i.e. for $P_G < P < P_A$, the system is locally stable. At P_G there exist two equilibrium states, one globally stable at point **G** and one unstable at point **C**. Furthermore, three equilibrium solutions exist at P_H , two locally stable (points **H** and **D**) and unstable at **B**. Consider now a straight column at equilibrium state **H**. A sufficient finite disturbance may cause the column to pass from **H** to locally stable state **D**. It should be noted that the * designated part of the characteristic curve is chosen to emphasize that even a small (small but not an infinitesimal) disturbance is sufficient for a column to pass from the trivial (pre-critical) configuration to the buckled one located on **CDE** branch. In practice this means that the column may buckle well below the bifurcation buckling force $P_{\text{bif}} = P_A$. Finally, for $P \geq P_A$ there are two solutions, one unstable which corresponds to a straight column on **AKJ** branch and one globally stable, i.e. buckled column on **EFI** branch. For a column to jump from the unstable state **K** to the globally stable equilibrium state **F**, only infinitesimal disturbance needs to be applied, obviously. The global buckling load which is the upper limit load of neutral equilibrium state is therefore in this case $P_G = 5.256$ N. In addition, if we confine the largest disturbance which causes up to e.g. δ_B change in geometry, then the critical load is P_H .

As expected the loading and unloading paths differ which means that a hysteresis loop exists. For example, if an initially straight column is loaded with P , the column remains straight up to point **G**. Further increase in force P may result in a violent jump between the states, e.g. from state **H** to state **D** if a sufficient finite disturbance is applied or from **A** to state **E** if even an infinitesimal disturbance is applied, followed by **DEFI** or **EFI**, respectively. The unloading path is obtained if P is gradually decreased from **I**. The column follows the **IFEDC** states, if there is no finite disturbance applied. A further decrease in P results in a snap back to state **G**. At this point the limit-point buckling is observed. If a sufficient finite disturbance is applied on **EDC** branch, the column may snap to the state on **AHG** branch. Point **G** is naturally followed by point **0**.

In the second nonlinear case, cf. Fig. 7(c), the stability conditions are similar as in the linear case with one additional observation. At initial post-buckling, more

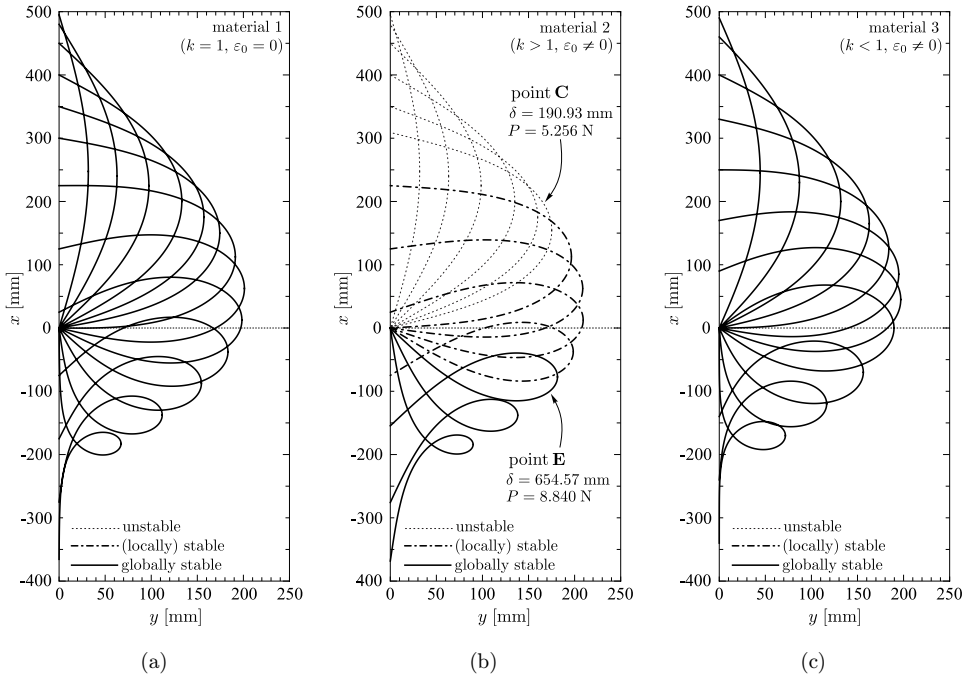


Fig. 8. Stable and unstable post-buckling shape modes for II Euler's case.

precisely at $**$ designated part of the characteristic curve, Fig. 7(c), a small increase in load P results in a rather small change of deformation δ . The column still bifurcates, i.e. the deformation still changes from purely axial contraction to lateral deflection. This means there is still a loss of stability, but there are no violent jumps between states. The critical buckling force is equal to the bifurcation load also in this case, $P_{cr} = P_A = P_{bif} = 1.109 \text{ N}$, but as can be seen from Fig. 7(c) there is practically no lateral deflection up to P^{**} .

Stable and unstable post-buckling shape modes for all three configurations of material constants are depicted in Fig. 8 for II Euler's case.

The influence of material on post-buckling shape modes of the hinged–hinged column can be observed in Fig. 9.

3.3. III Euler's case

Different and more complex results are obtained in the III Euler's case. Characteristic P – δ curves for this hinge–clamp supported column are shown in Fig. 10.

Stability conditions for the III Euler's case are less covered in the available literature. As can be found e.g. in Refs. 1 and 18–20 nonmonotonic P – δ curve of the nontrivial post-critical branch of solution is obtained in the linear case material one ($k = 1, \varepsilon_0 = 0$). It is illustrated also in Fig. 10(a) that P increases with δ in segment **ABC** and **HKLMNPRI**, but decreases in the **CDEFGH**. Bifurcation buckling

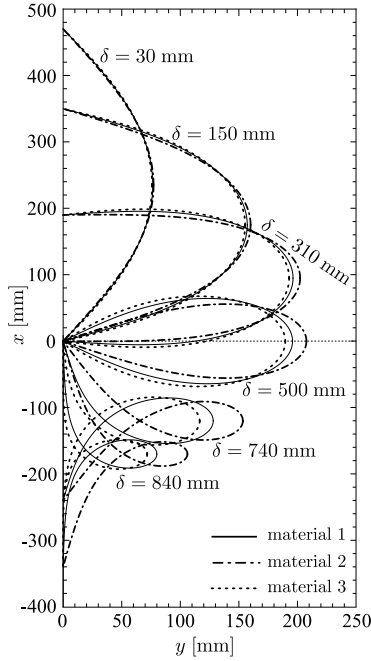


Fig. 9. Comparison of post-buckling shape modes for II Euler's case.

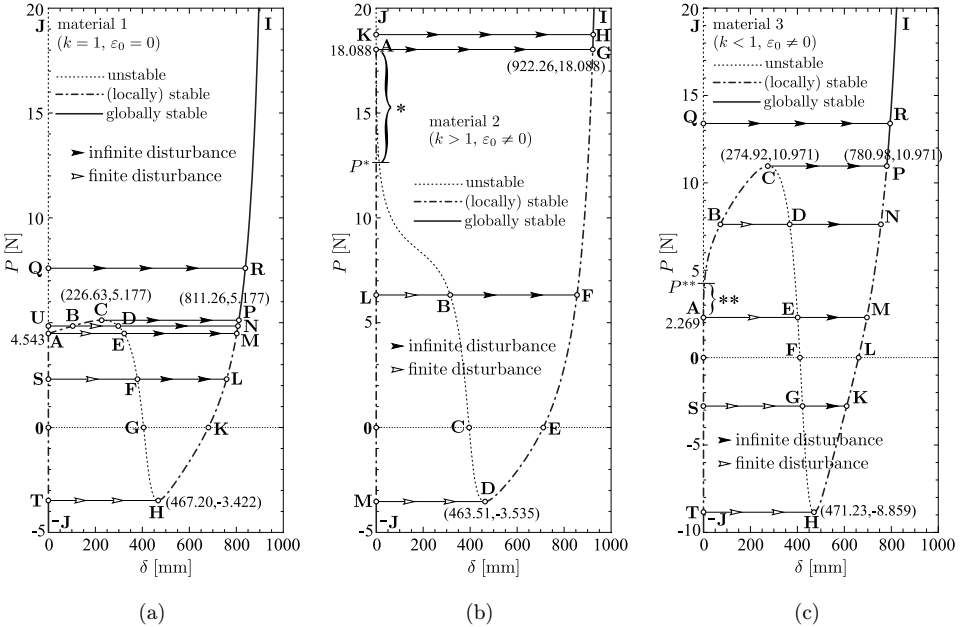


Fig. 10. Characteristic P - δ curves for III Euler's case.

force $P_{\text{bif}} = P_A = 4.543 \text{ N}$ is found at bifurcation point **A** which divides the curve of equilibrium states into the unstable branch **(A)UQJ** (trivial solution) and the branch which is locally stable on the **AB(C)** and **(H)KLMN(P)** segments, unstable on **CDEFGH** and globally stable on the **PRI** segment. Points **C** and **H** are the local maximum and minimum of the $P-\delta$ curve, respectively. It should be emphasized that the pre-critical sub-domain **-JTOSA** is in neutral state only for $P < P_T = -3.422 \text{ N}$, i.e. in **-J(T)** segment. Thus the (global) stability analysis may be important (in view of finite-disturbance buckling) even in the case when load P is tensile. In segment **(T)OSA**, i.e. for $P, P_T < P \leq P_A$, the system is only locally stable since for P_S there exist three equilibrium states, two locally stable **S, L**, and one unstable **F**. This means a sufficient finite disturbance may cause the column to buckle from state **S** to **L**. At P_T two equilibrium states can be found, one globally stable at point **T** and one unstable at point **H**. Notice also that there exist four equilibrium configurations for $P, P_A < P < P_C$, and three equilibrium configurations for $P = P_C$. The equilibrium state at point **U** is unstable which means that an infinitesimal disturbance causes the column to pass to a locally stable state at point **B**. Furthermore, if a sufficient (finite) disturbance is applied the column jumps to a locally stable state at **N**; or if the load is (quasistatically) increased (just infinitesimally) beyond the limit-point load P_C the column jumps to a globally stable equilibrium state at point **P**, i.e. a limit-point buckling is observed. For $P > P_C$ there exist only two solutions, one unstable on **(A)UQJ** branch and one globally stable on **PRI** branch. The column jumps at an infinitesimal disturbance from **Q** to **R**. Notice also that the states at **G** and **K** have both zero value P which means the horizontal reactive force alone is sufficient to maintain the static equilibrium of the column.

It is obvious that a hysteresis loop exists also in the III Euler's case since loading-unloading paths are different. For example if load P is applied and quasistatically increased from **0**, the column remains straight until the bifurcation buckling load is reached in state **A**, then it deforms through states **ABC**. Since **C** is a limit point, a further increase of P results in a snap-through to state **P** and the states of the column then follow the branch **PRI**. The loading path is thus **OSABCPRI**. On the other hand, the unloading path, which is obtained if the load is quasistatically decreased from **I**, is different. At first it follows **IRPNMLKH** branch and in **H** snaps-through to state **T**. Notice that P is now quite large and negative and the column is straight. There can be many different hysteresis loops found if we also take finite disturbances into consideration, e.g. loading path **OSLMNPRI**, and unloading path **IRPNBASO** if a finite disturbance is applied in **S** when loading and in **N** when unloading or similarly **OSABNPRI** and **IRPNMLS0** for that matter.

The stability conditions in a nonlinear case, where material 2 ($k > 1, \varepsilon_0 \neq 0$) is discussed, see Fig. 10(b), are similar as in I Euler case, material 2. The only difference is the negative value of the load P for δ , $\delta_C < \delta < \delta_E$. The part of the characteristic curve marked with * and therefore the need for introducing finite disturbances into the analysis is even more obvious here. Namely, the column may buckle, like already mentioned, well before the bifurcation buckling force is reached when disturbed by

small disturbance. Therefore $P_{cr} \leq P_A = P_{bif} = 18.088 \text{ N}$. Notice only one limit-point **D** is found on $P-\delta$ curve in this case in contrast to III Euler, material 1. The upper limit load of neutral equilibrium state is now $P_D = -3.535 \text{ N}$, which means the column subjected to a tensile load. In this case, practical evaluation of the critical buckling force which is in generally closely connected with largest disturbances would be e.g. P^* , cf. Fig. 10(b).

In the second nonlinear case, material 3 ($k < 1, \varepsilon_0 \neq 0$) cf. Fig. 10(c), the stability conditions are again similar as in the linear case with the same additional observation. At initial post-buckling, more precisely at $**$ designated part of the characteristic curve, cf. Fig. 10(c), a small increase in load P results in a rather small change of deformation δ . Again, no violent jumps between states are observed at initial post-buckling sub-domain up to point **C** where snap-through occurs. The critical buckling force is equal to the bifurcation load also in this case, $P_{cr} = P_{bif} = P_A = 2.269 \text{ N}$, but as can be seen from Fig. 10(c) there is practically no lateral deflection up to P^{**} .

From comparison of initial post-buckling segments of the diagrams for material 1 and material 2 in Fig. 10 one can perceive that at least one additional characteristically different $P-\delta$ curve exists. Within the limitations of the mathematical model proposed in this study an additional $P-\delta$ curve with local maximum has been found for III Euler’s case, material 2. The nontrivial post-critical branch of solution in Fig. 11(a) consists of two segments where $dP/d\delta < 0$, i.e. **AB** and **CD**, and two

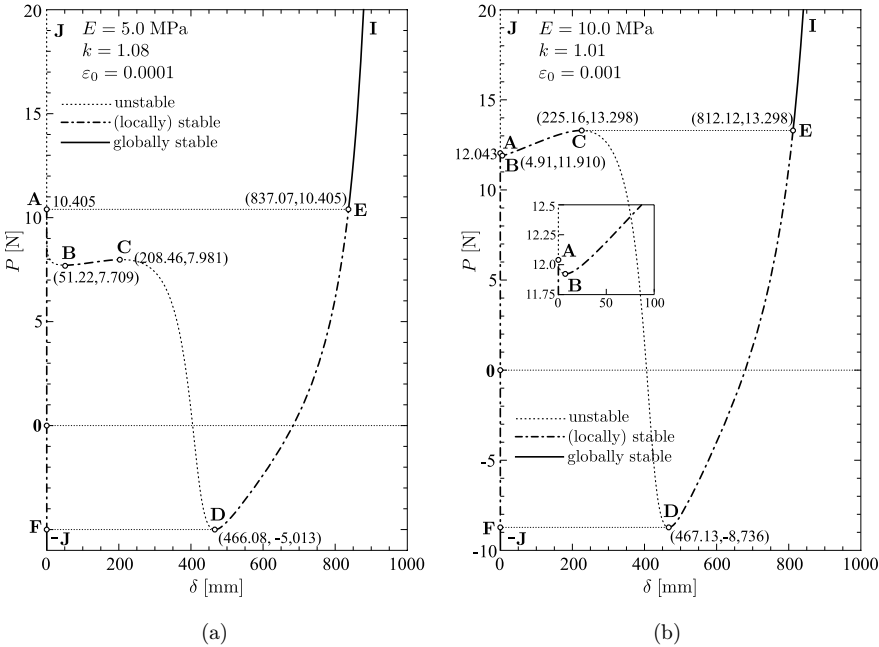


Fig. 11. Additional $P-\delta$ curves for III Euler’s case, material 2.

segments where $dP/d\delta > 0$, i.e. **BC** and **DEI**. From the detailed analysis given above we characterize segments **AB** and **CD** as unstable, segments **(B)(C)** and **(D)** **(E)** as (locally) stable, and the segment **EI** as globally stable. Similar observations can be written about the characteristic curve in Fig. 11(b). The main difference between both diagrams is that the lower limit of the globally stable segment in the second case is higher than bifurcation buckling load.

It should also be mentioned that even up to five different equilibrium solutions exist for a given load P , $P_B < P < P_C$ in Fig. 11(a) and for P , $P_B < P < P_A$ in Fig. 11(b).

Stable and unstable post-buckling shape modes for all three configurations of material constants are depicted in Fig. 12 for III Euler's case.

Post-buckling shape modes, depending upon the values of different material parameters involved, for this hinged–clamped column are shown in Fig. 13.

3.4. IV Euler's case

Results comparable to those in I and II Euler's cases are also obtained as expected for the IV Euler's case. Practically the same shapes of P – δ curves can be observed in Fig. 14 and therefore the same remarks can be applied. For columns of material 1, 2 and 3, the bifurcation buckling loads are $P_{\text{bif}} = 8.883$ N, $P_{\text{bif}} = 35.362$ N and $P_{\text{bif}} = 4.436$ N, respectively.

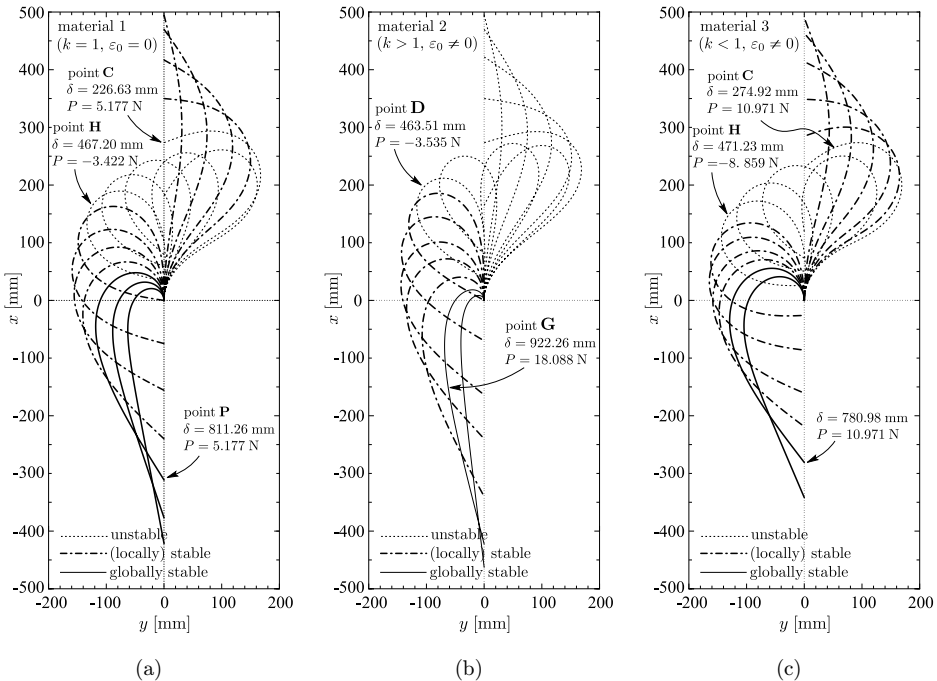


Fig. 12. Stable and unstable post-buckling shape modes for III Euler's case.

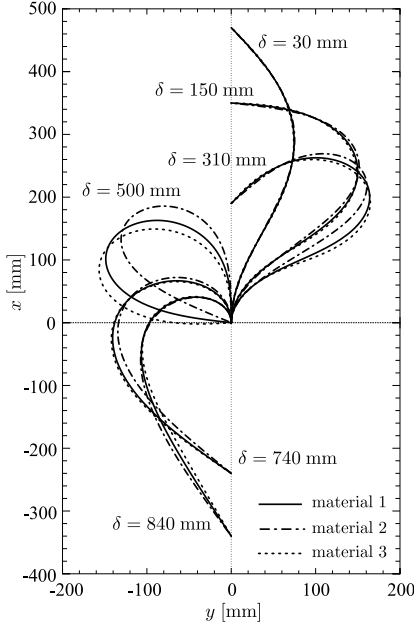


Fig. 13. Comparison of post-buckling shape modes for III Euler's case.

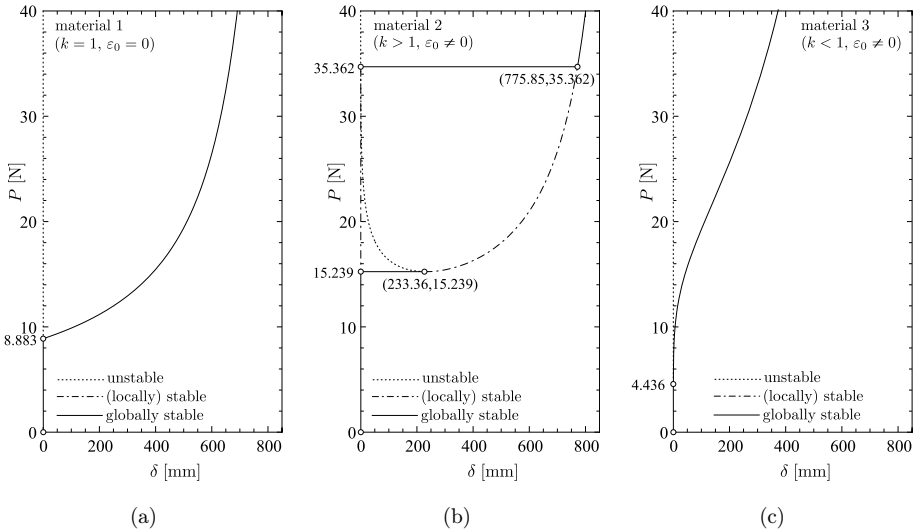


Fig. 14. Characteristic P – δ curves for IV Euler's case.

Stable and unstable post-buckling shape modes for all three configurations of material constants are depicted in Fig. 15 for IV Euler's case.

The influence of material on post-buckling shape modes of the clamp–clamp supported column can be observed in Fig. 16.

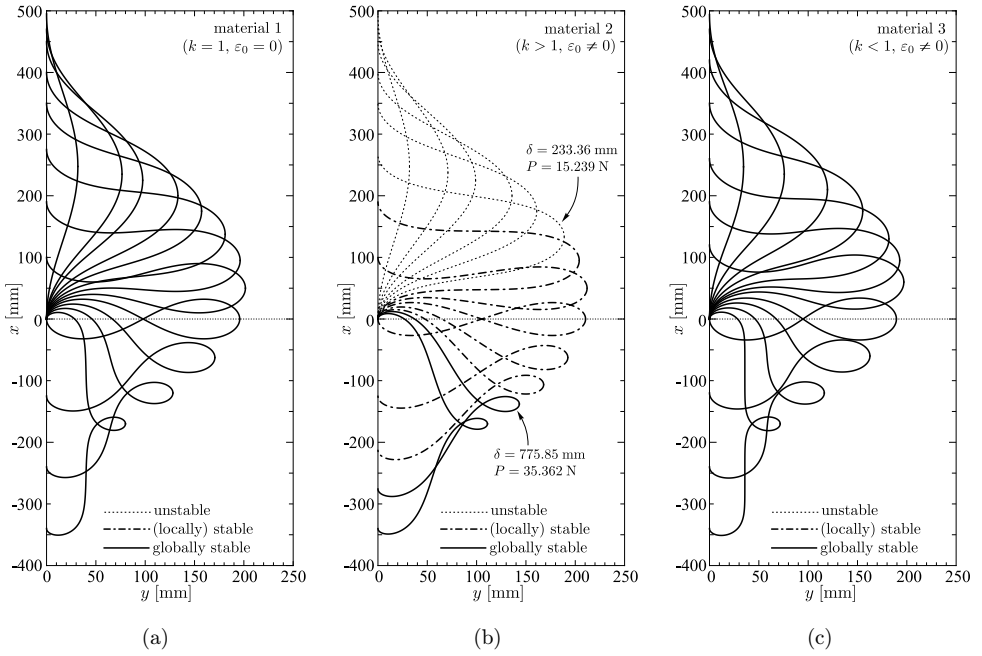


Fig. 15. Stable and unstable post-buckling shape modes for IV Euler's case.

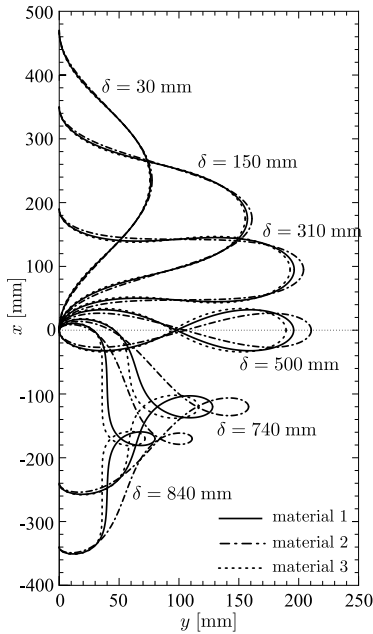


Fig. 16. Comparison of post-buckling shape modes for IV Euler's case.

Some remarks. Numerically obtained bifurcation buckling forces for all four Euler cases have the same values as those obtained via formulas for P_{bif} , which can be found in Table 1.

It should also be noted that only solutions for positive y values are taken into consideration in this article, cf. Figs. 4, 7, 10, 11, and 14. If both branches, obtained for $+y$ and $-y$, were considered simultaneously, then there would not be any globally stable equilibrium states (as we classified it in post-critical sub-domain) but only (locally) stable states.

To emphasize, the main practical applicability of our study is when disturbances are of finite proportions. In real engineering practice this means that equilibrium states e.g. in Fig. 10(b) for $P, P^* \leq P \leq P_A$, are “practically unstable” and part of the solution branch where $P_M \leq P \leq P_L$ is “practically stable”.

4. Conclusion

It is generally well-known that under the same boundary conditions multiple configurations can exist in nonlinear systems. Identifying and analyzing these configurations is often of crucial importance, especially when studying slender or thin-walled systems. In the proposed study stability and post-buckling configurations of slender uniaxial structural elements which could be made from natural rubber or any other material which obeys the modified Ludwick’s constitutive model were investigated. It should be emphasized that results obtained can be useful in engineering practice. Namely, in classical definition of structural stability only infinitesimal disturbances (small perturbations) are employed and therefore only stable and unstable states are recognized because the analysis is confined to a local region. But, as shown in this contribution, this is not enough since e.g. the column may buckle way below the bifurcation buckling force even when disturbed by small disturbance — therefore $P_{\text{cr}} \leq P_{\text{bif}}$. The value of critical buckling load P_{cr} which depends on the largest disturbance involved can be calculated numerically. The general mathematical formula for the global buckling load of columns made of modified Ludwick’s material is yet to be determined.

References

1. C. Y. Wang, Post-buckling of a clamped-simply supported elastica, *Int. J. NonLinear Mech.* **32**(6) (1997) 1115–1122.
2. S. N. Korobeinikov, Secondary loss of stability of a simply supported rod, in *Proc. 4th Int. Conf. Laurent’ev Readings on Mathematics, Mechanics, and Physics* (Novosibirsk, Russia, 1995), p. 104.
3. V. V. Kuznetsov and S. V. Levyakov, Secondary loss of stability of an Euler rod, *J. Appl. Mech. Tech. Phys.* **40**(6) (1999) 1161–1162.
4. V. V. Kuznetsov and S. V. Levyakov, Elastica of an Euler rod with clamped ends, *J. Appl. Mech. Tech. Phys.* **41**(3) (2000) 544–546.
5. S. V. Levyakov, States of equilibrium and secondary loss of stability of a straight rod loaded by an axial force, *J. Appl. Mech. Tech. Phys.* **42**(2) (2001) 321–327.

6. V. V. Kuznetsov and S. V. Levyakov, Complete solution of the stability problem for elastica of Euler's column, *Int. J. NonLinear Mech.* **37**(6) (2002) 1003–1009.
7. B. Wu, Secondary buckling of an elastic strut under axial compression, *ZAMM — Z. Angew. Math. Mech.* **75**(10) (1995) 741–751.
8. B. Wu, Secondary buckling of an elastic column with spring-supports at clamped ends, *Arch. Appl. Mech.* **68**(5) (1998) 342–351.
9. B. Wu, Secondary buckling of an elastic column with a central elastic support, *Mech. Res. Commun.* **25**(4) (1998) 479–486.
10. C. Y. Wang, Global buckling load of a nonlinearly elastic bar, *Acta Mech.* **119**(1–4) (1996) 229–234.
11. T. J. Kang, K. H. Joo and K. W. Lee, Analyzing fabric buckling based on nonlinear bending properties, *Tex. Res. J.* **74**(2) (2004) 172–177.
12. J. H. Jung and T. J. Kang, Large deflection analysis of fibers with nonlinear elastic properties, *Tex. Res. J.* **75**(10) (2005) 715–723.
13. M. Brojan, A. Puksic and F. Kosel, Buckling and postbuckling of a nonlinearly elastic column, *ZAMM — Z. Angew. Math. Mech.* **87**(7) (2007) 518–527.
14. M. Brojan and F. Kosel, Approximative formula for post-buckling analysis of nonlinearly elastic columns with superellipsoidal cross-sections, *J. Reinf. Plast. Compos.* **30**(5) (2011) 409–415.
15. M. Brojan, T. Videnic and F. Kosel, Large deflections of nonlinearly elastic non-prismatic cantilever beams made from materials obeying the generalized Ludwick constitutive law, *Meccanica* **44**(6) (2009) 733–739.
16. G. J. Simitses and D. H. Hodges, *Fundamentals of Structural Stability*, 1st edn. (Elsevier Inc., Burlington, MA, 2006).
17. J. H. Maddocks, Stability and folds, *Arch. Ration. Mech. Anal.* **99**(4) (1987) 301–328.
18. M. A. Vaz and D. F. C. Silva, Post-buckling analysis of slender elastic rods subjected to terminal forces, *Int. J. NonLinear Mech.* **38**(4) (2003) 483–492.
19. B. Phungpaingam and S. Chucheepsakul, Post-buckling of an elastic column with various rotational end restraints, *Int. J. Struct. Stab. Dyn.* **5**(1) (2005) 113–123.
20. S. V. Levyakov and V. V. Kuznetsov, Stability analysis of planar equilibrium configurations of elastic rods subjected to end loads, *Acta Mech.* **211**(1–2) (2010) 73–87.